Effect of the coupling beam with different intensity profile upon Rydberg EIT and Rydberg two-color polarization spectroscopy with Cesium ladder-type level

Rui Chang, Tao Wang, Yuhui Yang, Lili Hao, Jun He, and *Junmin Wang**

Rui Chang, Tao Wang, Yuhui Yang, Lili Hao, Jun He, Junmin Wang
State Key Laboratory of Quantum Optics and Quantum Optics Devices, and Institute of Opto-Electronics
Shanxi University
Tai Yuan 030006, China
Email: wwjjmm@sxu.edu.cn
Jun He, Junmin Wang
Collaborative Innovation Center of Extreme Optics
Shanxi University
Tai Yuan 030006, China

Electromagnetically induced transparency (EIT) and two-color polarization spectroscopy (TCPS) with Rydberg atoms are spectroscopic techniques developed based on the interaction between a ladder-type three-level atomic system and two light fields. The narrow linewidth and high contrast Rydberg EIT and Rydberg TCPS have important applications in laser frequency stabilization, Rydberg antennas, Rydberg radar and detecting microwave electric fields. Here, the EIT and TCPS with cesium Rydberg atoms have been investigated using a ladder-type level system driven by the 509-nm coupling beam and the 852-nm probe beam. The 509-nm coupling beam with three kind of intensity spatial profile (Laguerre–Gaussian mode, TEM_{00} Gaussian mode, Flat-top mode) is employed one by one in experiments. Due to the different intensity spatial distributions of the three 509-nm coupling beams, the Autler-Townes (A-T) splitting method is utilized to calibrate the Rabi frequency of the coupling beams. Our results show that the linewidth is narrowest when the 509-nm coupling beam has the Laguerre-Gaussian mode with equal Rabi frequency among the three cases, we optimized the linewidth and contrast of the EIT and TCPS by varying the beam sizes of the 509-nm Laguerre-Gaussian beams. The laser frequency stabilization by using of TCPS with three kinds of 509-nm coupling beams are compared, the Laguerre-Gaussian coupling beam case is more effective for frequency stabilization because of the narrower linewidth.

1 Introduction

In recent years, the Rydberg atoms have attracted much attention because of their long lifetime, large electric dipole moment, huge polarizability, and strong long range interaction. Based on the interaction between Rydberg atoms and the light field, a variety of spectroscopic techniques have been developed, such as Rydberg electromagnetically induced transparency (EIT) and two-color polarization spectroscopy (TCPS). EIT is the typical quantum interference phase cancellation effect produced by the interaction of light and matter, which is based on the principle of introducing a controlled laser field to produce the interference phase cancellation effect between atomic quantum states and effectively suppressing the resonance absorption of the probe beam. The concept of EIT was first introduced by S.E. Harris in 1990 [1], and the following year the EIT phenomenon was observed in Sr and Pb atomic gases by S.E. Harris' group [2, 3]. Since then, numerous research groups have carried out a great deal of theoretical and experimental research based on EIT [4, 5, 6, 7, 8]. In 1995, M. Xiao group observed the EIT phenomenon in a three-level ladder-type and Λ-type thermal Rb atomic gas and effectively eliminated the first-order Doppler effect in the system [9]. In 2007, C.S. Adams group, made non-destructive measurements of Rb atoms in the Rydberg state using the EIT technique [10]. Rydberg EIT is gradually coming into the spotlight, both to exploit the long-range interactions between Rydberg atoms and to use EIT to reduce irreversible optical losses due to absorption, while simultaneously slowing down the group velocity of the signal photons. Rydberg EIT has a wide range of applications in laser frequency stabilization [11], non-destructive probing[10], precise measurement of energy levels and lifetimes of Rydberg atoms [12], quantum storage [13], and precision measurement of microwave electric fields [14].

TCPS is based on laser-induced dichroism and birefringence to induce nonlinear saturation absorption effects in atomic gas medium to obtain high-resolution spectra without Doppler background [15]. In ad-

dition to the advantages of traditional spectroscopic techniques, it is characterized by high sensitivity and high resolution. It is widely used in laser frequency stabilization, combustion diagnostics, quantum frequency scales, etc. In 2000, H. B. Lu et al. in Ti sapphire laser frequency stabilization experiments, Rb atomic polarization spectral line as a frequency discrimination line, compared with the use of saturated absorption spectroscopy has the advantages of fast response speed, high sensitivity, and simple and practical feedback circuits [16]. In 2011, J. Wang et al. compared the frequency stabilization of the 780-nm diode laser using the saturated absorption spectroscopy of Rb atoms and the polarized spectroscopy, respectively, and found that the polarized spectrum without modulation can significantly improve the long-term laser frequency stability [17]. In 2014, H. F. Liu et al. used the TCPS technique to lock a laser at the wavelength of 1529 nm to the $5P_{3/2}(F'=3)-4D_{5/2}(F''=4)$ transition of Rb [18]. In 2022, N. Duarte Gomes et al. used Laguerre-Gaussian beams and Gaussian beams, as the coupling beam, respectively, to produce Rydberg TCPS, directly measured the linewidths of the EITs and compared them [19].

Linewidth and contrast are important parameters of EIT spectra, and narrow EIT spectra have a direct impact on the group velocity of the probe beam for realizing quantum storage and have applications in precision measurements [20, 21]. It is well known that reducing the intensity of beam can reduce the effect of power broadening and narrow the spectrum, but at the same time, it will reduce the contrast. It has been shown that the use of Laguerre-Gaussian beams as the coupling beams in hot Rb atomic vapors [22, 23, 24] and ultracold Rb atoms[25, 26] can reduce the EIT linewidths due to the spatial distribution of the intensity as compared to the Gaussian beams.

In this paper, we use three kind of 509-nm coupling beams (Laguerre–Gaussian mode, TEM_{00} Gaussian mode, Flat-top mode), and TEM_{00} Gaussian mode the 852-nm probe beam interacted with cesium ladder-type three-level system with Rydberg atom to obtain the Cs Rydberg-EIT and TCPS. First, we simulate the dispersion curves of the EIT for the ladder-type three energy level systems and obtain the spectra experimentally. Second, due to the different spatial intensity distributions of the three beams, and to ensure that the light-atom interactions have the same intensity, we used the A-T splitting method to calibrate the Rabi frequency of the three beams, we obtained the EIT and TCPS using the 852 nm+509 nm and compared the EIT and TCPS linewidths of the coupling beam for the three spatial modes at the same Rabi frequency. The EIT linewidth is narrower when the coupling beam is the Laguerre–Gaussian mode, and we optimize the spectrum by changing the size of the Laguerre-Gaussian beam. Finally, the TCPS can be used for 509 nm frequency locking, and since the EIT linewidths of the three beams are different, we compared their frequency stability respectively.

2 Experimental setup and theory

2.1 Experimental setup

Figure 1 shows the Rydberg ladder-type three-level system $(6S_{1/2}-6P_{3/2}-52S_{1/2})$. The P-polarized 852 nm probe beam is locked to the $6S_{1/2}(F=4)-6P_{3/2}(F'=5)$ transition of the Cs polarization spectrum. Circularly polarized 509 nm coupling beam scanned over the $6P_{3/2}(F'=5)-52S_{1/2}$ transition. TCPS is produced by linearly polarized 852 nm and circularly polarized 509 nm, and the Cs vapor follows the Maxwell-Boltzmann distribution at room temperature, which is uniformly distributed among the different Zeeman states of the ground state $6S_{1/2}(F=3, 4)$, the atoms are excited to the $52S_{1/2}$ Rydberg state by the combination of 852 nm linearly polarized light and 509 right nm circularly polarized light, the atoms spontaneously radiate into the $6P_{3/2}(F'=5, m_F=4,5)$, causing the non-uniform distribution on the Zeeman states, and the Cs vapor turns into an anisotropic medium. The linearly polarized probe beam can be considered a combination of left-rotated and right-rotated circular polarization, their refractive index coefficients are different when they propagate in anisotropic media, so that the 852nm polarization changes, then into a balanced photodetector, which converts the optical signal into an electrical signal to obtain the TCPS.

Figure 2 shows the experimental setup, the probe beam is generated by Toptica DL Pro@852 nm laser,
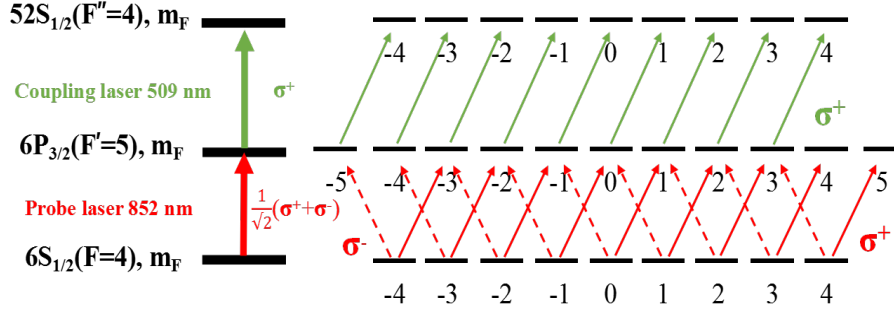
Figure 1: Schematic of the Rydberg ladder-type three level system ($6S_{1/2}$-$6P_{3/2}$-$52S_{1/2}$). The probe beam is linearly polarized and the coupling beam is circularly polarized. The 852 nm probe beam is locked to the $6S_{1/2}$(F=4)-$6P_{3/2}$(F'=5) transition, and the 509 nm coupling beam frequency is scanned over the $6P_{3/2}$(F'=5)-$52S_{1/2}$. The 509 nm right circularly polarized beam passes through Cs vapor, causing the non-uniform distribution on the Zeeman states, and the Cs vapor turn into an anisotropic medium, the 852nm linearly polarized beam can be regarded as a combination of σ^+ and σ^-, and when passing through the anisotropic medium, the refractive indices of the left and right polarization components are different, so that the 852nm polarization changes and TCPS is obtained by using a balanced photodetector.

after the PBS, one beam is used for the polarization spectrum to lock the 852 nm frequency, and the other beam is used for performing EIT and TCPS with Cs Rydberg atoms.
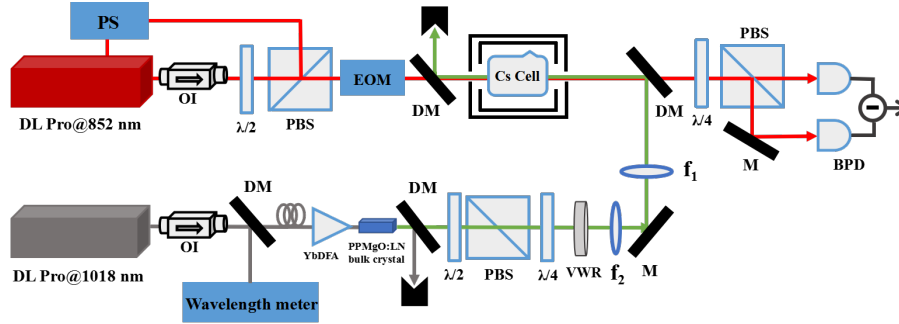

Figure 2: Experimental setup diagram. PBS: polarization beam splitter cube; $\lambda/2$: half wave plate; $\lambda/4$: quarter wave plate; OI: optical isolator; EOM: electro-optical modulator; YbDFA: ytterbium-doped fiber amplifier; DM: dichroic mirror; VWR: vortex wave retarder plate; BPD: balanced photodetectors, PS: polarization spectroscopic device, P_{probe}=23 μW, w_{probe}=5.8 mm, $w_{coupling}$ varies with the f_1 and f_2

2.2   Theoretical model

For the ladder-type three level system in Fig. 1, we consider $6S_{1/2}$, $6P_{3/2}$, $52S_{1/2}$ as $|1\rangle$, $|2\rangle$, $|3\rangle$. We use the density matrix to simulate the three level system, the equation for the evolution of the density matrix over time is given by:

$$\dot{\rho} = -\frac{i}{\hbar}[H, \rho] + \hat{\mathcal{L}}(\rho), \tag{1}$$

H is the Hamiltonian of the system after considering the spin wave approximation, $\hat{\mathcal{L}}(\rho)$ includes attenuation and decoherence factors in the ladder-type three energy level systems, H and $\hat{\mathcal{L}}(\rho)$ the matrix form can be expressed as:

$$H = \frac{\hbar}{2}\begin{pmatrix} 0 & \Omega_p & 0 \\ \Omega_p & -2\Delta_1 & \Omega_c \\ 0 & \Omega_c & -2(\Delta_1 + \Delta_2) \end{pmatrix}, \tag{2}$$

$$\hat{L}(\rho) = \begin{pmatrix} \Gamma_{21}\rho_{22} & -\frac{\Gamma_{21}}{2}\rho_{12} & -\frac{\Gamma_{32}}{2}\rho_{13} \\ -\frac{\Gamma_{21}}{2}\rho_{21} & -\Gamma_{21}\rho_{22} + \Gamma_{32}\rho_{33} & -\frac{\Gamma_{21}+\Gamma_{32}}{2}\rho_{23} \\ -\frac{\Gamma_{32}}{2}\rho_{31} & -\frac{\Gamma_{21}+\Gamma_{32}}{2}\rho_{32} & -\Gamma_{32}\rho_{33} \end{pmatrix}, \tag{3}$$

Where Γ_{ij} is the spontaneous radiance from energy levels i to j, The density matrix element on the diagonal denotes the probability of the particle population at the energy level, due to the probe beam is very weak, the probability of atomic transfer is very low, so

$$\rho_{11} \approx 1, \rho_{22} \approx \rho_{33} \approx 0,$$

An expression for the density matrix element associated with the probe beam absorption and dispersion can be obtained as:

$$\rho_{12} = \frac{i\Omega_p/2}{\Gamma_3/2 + \gamma_{rel} - i(\Delta_p^2 + k_p v_x + \Delta_c - k_c v_x) + \Gamma_2/2 + \gamma_p - i(\Delta_p + k_p v_x)}, \tag{4}$$

Ω_c, Ω_p are the Rabi frequency of the coupling beam, the probe beam, respectively

$$\Omega_p = \frac{\mu_{12}\varepsilon_{0,p}}{\hbar}, \quad \Omega_{c,G} = \frac{\mu_{23}\varepsilon_{0,c}}{\hbar} = \Omega_{0,c}, \quad \Omega_{c,LG} = \frac{\mu_{23}\varepsilon_{c,LG}}{\hbar} = \Omega_{0,c}\frac{\sqrt{2}r}{w_c}e^{-r^2/w_c^2},$$

Based on the $\mu_{21}N\rho_{21}(\omega_{\mathfrak{p}}) = \varepsilon_0\chi(\omega_{\mathfrak{p}})E_{\mathfrak{p}}$, the polarization rate χ can be obtained:

$$\chi = \frac{2N|\mu_{12}|^2}{\hbar\epsilon_0\Omega_p\sqrt{\pi}u} \int_{-\infty}^{+\infty} \rho_{12}e^{-v^2/u^2}dv, \tag{5}$$

The Im $[\chi]$ reflects the absorption of the probe beam by the medium, the Re $[\chi]$ reflects the dispersion of the medium to the probe beam [27],

$$Tr_p = e^{-Im[\chi]k_p l}, \quad S_G = \frac{k_p}{2}Re[\chi], \tag{6}$$

For the coupling of Laguerre-Gaussian modes, the polarizability needs to be integrated over the interaction region between the coupling beam at 509 nm and the probe beam at 852 nm [25], then the absorption and dispersion can be expressed as

$$Tr_p = \frac{2}{w_p^2} \int_0^{w_p} \exp\left(-Im[\chi]k_p l\right)rdr, \quad S_{LG} = \frac{2}{w_p^2} \int_0^{w_p} \frac{k_p}{2}Re[\chi]rdr. \tag{7}$$

Figure 3 shows the theoretically TCPS spectra as a function of Δc for the 509-nm Gaussian (red line) and Laguerre-Gaussian mode (blue line) coupling beams. $\Omega_c = 2\pi \times 3$ MHz, $\Omega_p = 2\pi \times 2$ MHz. In this case, the linewidth of TCPS is $\Delta\nu_G$=7.9 MHz and $\Delta\nu_{LG}$=6.2 MHz.
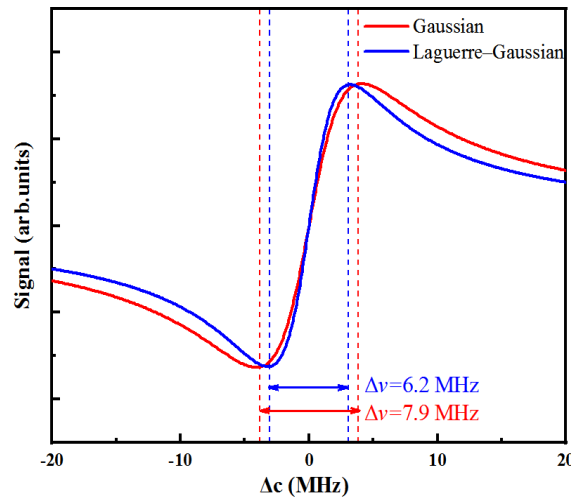

Figure 3: Theoretical simulation of TCPS. The 852-nm probe beam is a TEM$_{00}$-mode Gaussian beam, $\Omega_p = 2\pi \times 2$ MHz, and the 509-nm coupling beam is a TEM$_{00}$-mode Gaussian beam or Laguerre-Gaussian beam, $\Omega_c = 2\pi \times 3$ MHz, respectively. With these parameters, the simulated linewidths of TCPS are $\Delta\nu_G$=7.9 MHz ($\Delta\nu_{LG}$=6.2 MHz) for the 509-nm coupling beam with the TEM$_{00}$ Gaussian mode (the Laguerre-Gaussian mode).

3 Experimental results and analysis

3.1 Rydberg EIT and Rydberg TCPS

Figure 4 shows the Rydberg EIT and Rydberg TCPS spectra with the 852-nm TEM$_{00}$ mode Gaussian probe beam and the 509-nm TEM$_{00}$ mode Gaussian coupling beam driven ladder-type three-level Cs system with Rydberg state. The red line is the EIT signal, and the black line is the corresponding TCPS signal. We defined the frequency difference $\Delta\nu$ between the peak and the dip in TCPS signal as the linewidth of Rydberg TCPS. We experimentally confirm that the TCPS linewidth is equal to the EIT linewidth.
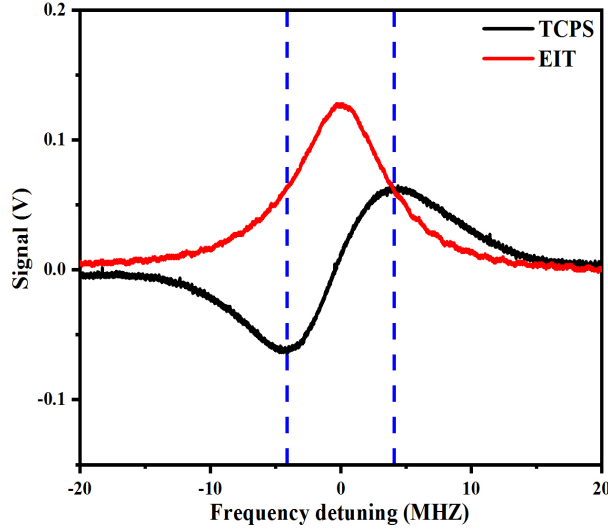

Figure 4: Typical Rydberg EIT signal (red) and Rydberg TCPS signal (black) of Cs ladder-type three-level system (6S$_{1/2}$-6P$_{3/2}$-52S$_{1/2}$) driven by 852-nm probe beam (locked to (F=4)-(F'=5) cycling transition) and 509-nm coupling beam. Both of the probe and coupling beams have Gaussian TEM$_{00}$-mode. $\Omega_c = 2\pi \times 3$ MHz, $\Omega_p = 2\pi \times 2$ MHz. The linewidth of the EIT signal and the TCPS signal is $\Delta\nu$=8.2 MHz.

3.2 Calibration of 509-nm coupling beam's Rabi frequency using A-T splitting

Experimentally, we use three kind of 509-nm coupling beams (Laguerre–Gaussian mode, TEM$_{00}$ Gaussian mode, Flat-top mode), and TEM$_{00}$ Gaussian mode the 852-nm probe beam interacted with cesium ladder-type three-level system with Rydberg atom to obtain the Cs Rydberg-EIT and TCPS. We use a vortex wave retarder (VWR) to obtain the Laguerre-Gaussian beam, the intensity distribution is shown in Fig. 5(a) and the flat-top beam we generate using a π-Shaper, the intensity distribution is shown in Fig. 5(b).

We compare the linewidth of EIT and TCPS for three kind of 509-nm coupling beams, and the factors affecting the linewidth are mainly the power broadening and the transition broadening. The power broadening mainly depends on the Rabi frequency of the beam, while the transition broadening mainly depends on the beam size. Due to the different spatial intensity distributions of the three beams, the method of defining the beam size is not uniform, it is well known that the size of the Gaussian beam takes the radial distance from the maximum intensity down to $1/e^2$, the intensity distribution of the flat-top beam is simpler, and its size takes the profile of the intensity distribution as the diameter, however, for the Laguerre-Gaussian beam, the intensity distribution is more complex, and we defined its size as the radial distance between the intensity maximum. According to this definition, we make their sizes equal, but define the sizes differently, so calculating the Rabi frequency of the three beams becomes difficult. For this problem, we adopt A-T splitting to calibrate the Rabi frequency of the three beams, fixing the size and power of the probe beam, fixing the size of the coupling beam, and increasing the power of the coupling beam, so that the EIT can generate A-T splitting under the strong coupling beam, and the

corresponding Rabi frequency is obtained according to the splitting distance. The results are shown in Fig. 6, where the Rabi frequency of the three coupling beams versus power with the same size.
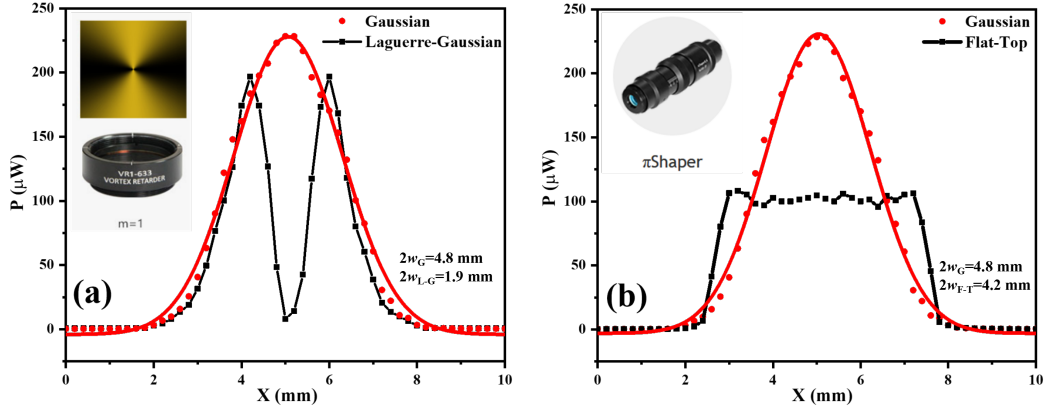

Figure 5: Three 509-nm coupling beams with different radial intensity distributions measured by the knife-edge method. (a) The Laguerre-Gaussian beam is generated through a vortex wave retarder (VWR) with m = 1, and the size is defined as the distance between the two peaks of intensity. (b) The flat-top beam is generated by a π-Shaper with uniform distribution of intensity, and the size is defined as the profile of the intensity distribution.
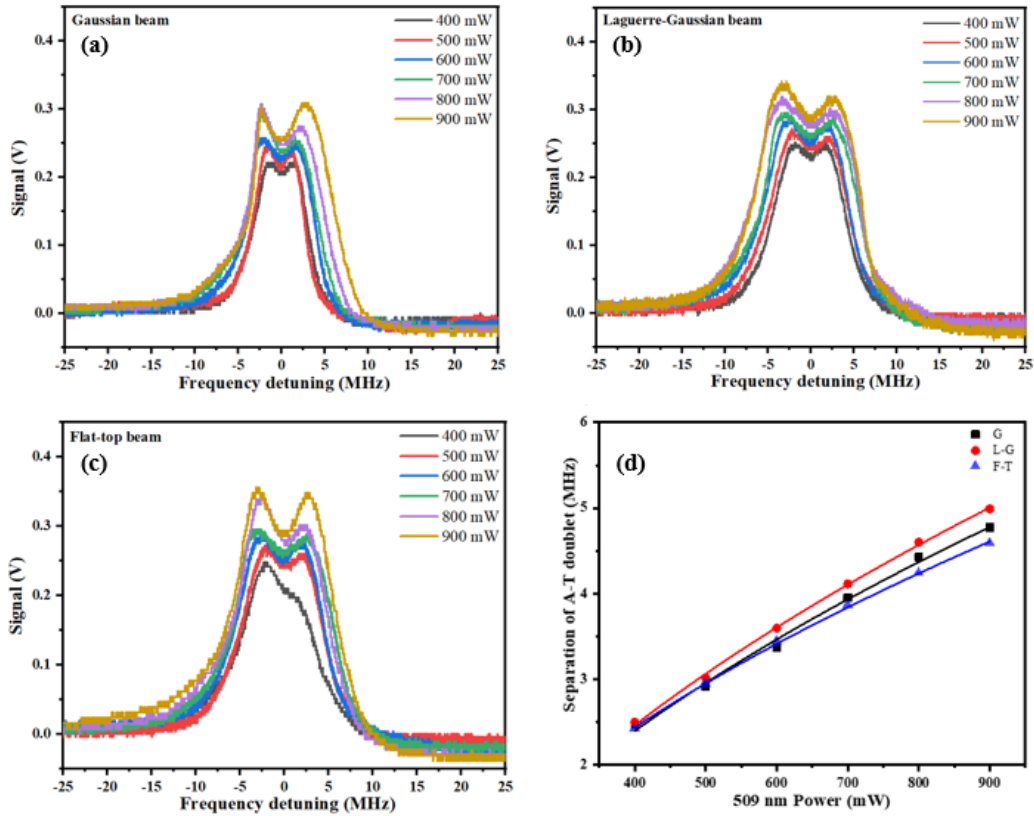

Figure 6: A-T splitting of the Rydberg EIT ($6S_{1/2}$-$6P_{3/2}$-$52S_{1/2}$), A-T splitting distance increases with increasing coupling beam power, and the A-T splitting is utilized to calibrate the Rabi frequency. (a) A-T splitting spectrum of the 509 nm for TEM_{00}-mode Gaussian beam. (b) A-T splitting spectrum of the 509 nm for Laguerre-Gaussian beam. (c) A-T splitting spectrum of the 509 nm for flat-top beam. (d) The A-T splitting interval as a function of power for three beams with different radial intensity distributions.

3.3   Rydberg TCPS with three kinds of 509-nm coupling beam with different spatial intensity distributions

By the method of A-T splitting, we obtained the relation between Rabi frequency and power for three kind of 509-nm coupling beams. We selected three beams with coupling Rabi frequency $\Omega_c = 2\pi \times 3$ MHz, and the TEM$_{00}$-mode Gaussian probe beam is $\Omega_p = 2\pi \times 2$ MHz to make the TCPS, and compared their linewidths, as shown in Fig. 7, the results indicate that the narrowest linewidth is obtained when Laguerre-Gaussian beam is used as the coupling beam. This result is due to the spatial intensity distribution of the beam, when the coupling beam is in Laguerre-Gaussian mode, the intensity of its central region is almost zero, the interaction region with the Gaussian probe beam is reduced and the interaction with the central region of maximum intensity is weakened, the optical pumping effect in the EIT spectrum is reduced, making the linewidth narrower. Using this spatial mode of the beam, the EIT linewidth can be reduced without significantly decreasing the amplitude.
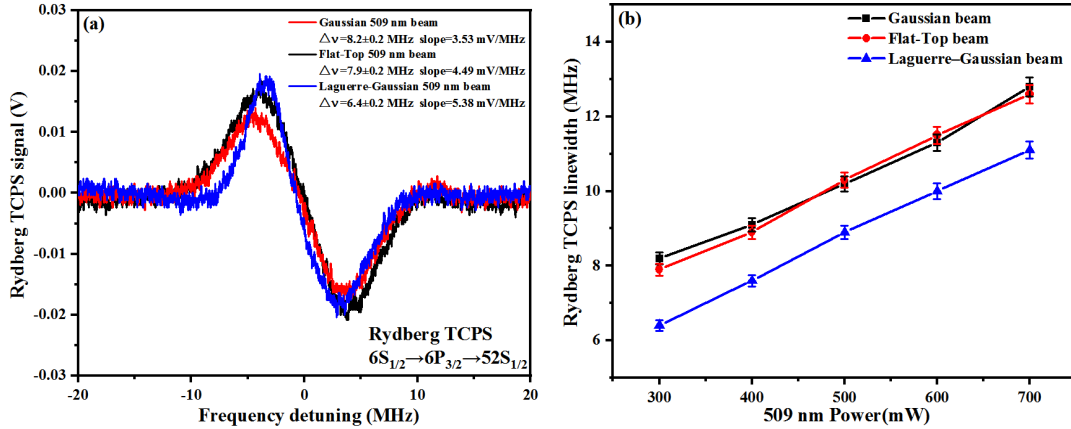

Figure 7: Rydberg TCPS with the 509-nm beam for three different spatial intensity distributions. (a) Linewidths of the Rydberg TCPS are compared by changing the spatial modes of the 509-nm coupling beam, fixed $\Omega_c = 2\pi \times 3$ MHz, and the 852-nm TEM$_{00}$-mode Gaussian beam $\Omega_p = 2\pi \times 2$ MHz, with $\Delta\nu$=8.2 MHz for the 509-nm TEM$_{00}$-mode Gaussian beam, $\Delta\nu$=7.9 MHz for the 509-nm flat-top beam, and $\Delta\nu$=6.4 MHz for the 509-nm Laguerrean-Gaussian beam. By comparison, the TCPS linewidth is narrowest when 509 nm is the Laguerre-Gaussian beam, and this result is due to changing the spatial structure of the coupling beam. (b) The Rydberg TCPS linewidths of the three beams with different spatial intensity distributions broaden with increasing the 509 nm power, the narrowest linewidth when 509 nm is the Laguerre-Gaussian beam.

Table 1: The parameters of f_1 and f_2 used to change the beam size

Laser beam	f_1 (mm)	f_2 (mm)	Beam diameter (mm)
Probe@852 nm	50	50	6.1
Coupling@509 nm	without lens	without lens	0.8
Coupling@509 nm	20	50	2.1
Coupling@509 nm	20	90	3.7
Coupling@509 nm	20	150	6.3
Coupling@509 nm	20	200	7.9
Coupling@509 nm	20	250	10.1

The results show that the Laguerre-Gaussian beam as coupling beam obtains the narrowest linewidth of the EIT, which is due to its unique spatial intensity distribution and Gaussian beam interaction region, so we experimentally change the area of its central region with the combination of two lenses to optimize the spectrum. Table 1 shows the parameters of f_1 and f_2, and Fig. 8 shows the optimization results of the spectra with different sizes of 509 nm. The results show that even though there are differences in the spatial intensity distributions of the Laguerre-Gaussian coupling beam and the TEM$_{00}$-mode Gaussian probe beam, when the sizes are approximately equal, the EIT has narrow linewidths and large contrasts. We optimized the TCPS spectra at the same time as we optimized the EIT spectra, and the narrow linewidth-high-contrast EIT has important applications in the field of precision measurements.
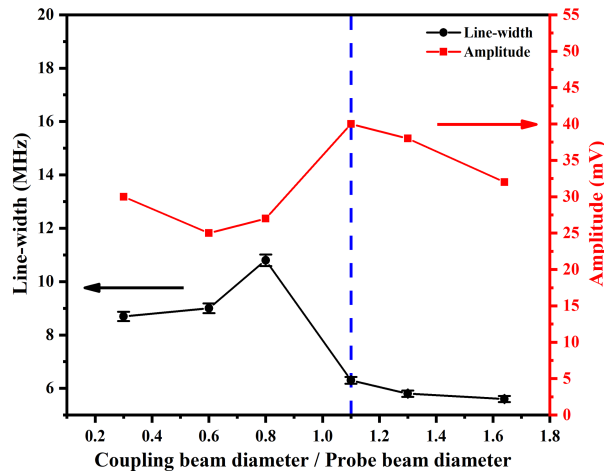
Figure 8: Optimization of the TCPS by changing the Laguerre-Gaussian beam size. The TCPS linewidth $\Delta\nu$ varies with the 509-nm Laguerre-Gaussian beam size. The 509-nm Laguerre-Gaussian beam size increases gradually, while the linewidth becomes narrower. The results show that even though there are differences in the radial intensity distributions of the 509-nm Laguerre-Gaussian coupling beam and the 852-nm TEM$_{00}$-mode Gaussian probe beam, when the sizes are approximately equal, the EIT has narrow linewidths and large contrasts.

3.4   Frequency stabilization of the 509-nm laser by using of Rydberg TCPS

Electromagnetically induced transparency (EIT) is typically modulated and demodulated to obtain a first-order differentiated signal that can be used for laser frequency locking. However, this method can introduce additional noise due to the modulation and demodulation processes. In contrast, the TCPS method used in this manuscript is an unmodulated approach. The TCPS has a very large dispersion at the resonance, so it is suitable for locking the laser frequency to the atomic transition, TCPS exploits the optical anisotropy induced by circularly or linearly polarized beams in the medium to achieve high-resolution spectra without Doppler broadening. [28].

Before locking the frequency of the 509 nm laser, it is necessary to first lock the frequency of the 852 nm laser. The residual frequency fluctuations of the 852 nm laser can potentially affect the frequency stability of the 509 nm laser after it is locked using TCPS. In our experiment, we first locked the 852 nm laser in the polarization spectrum of the 6S$_{1/2}$(F=4)-6P$_{3/2}$(F′=5) transition and recorded its residual frequency fluctuation for 30 minutes using a digital multimeter, resulting in 0.54 MHz. This residual fluctuation is relatively small and does not significantly impact the subsequent frequency stabilization of the 509 nm laser, as demonstrated by the TCPS measurements. After the 852 nm frequency is locked, the 509 nm laser frequency is locked using the TCPS, and the linewidth and contrast of the EIT determine the slope of the TCPS at the resonance. In the experiment, the 509 nm laser is locked to three beams with different slopes of TCPS to compare the frequency stability after frequency locking, and the results show that the larger slope of the TCPS, the better frequency stabilization, the results are shown in Fig. 9.
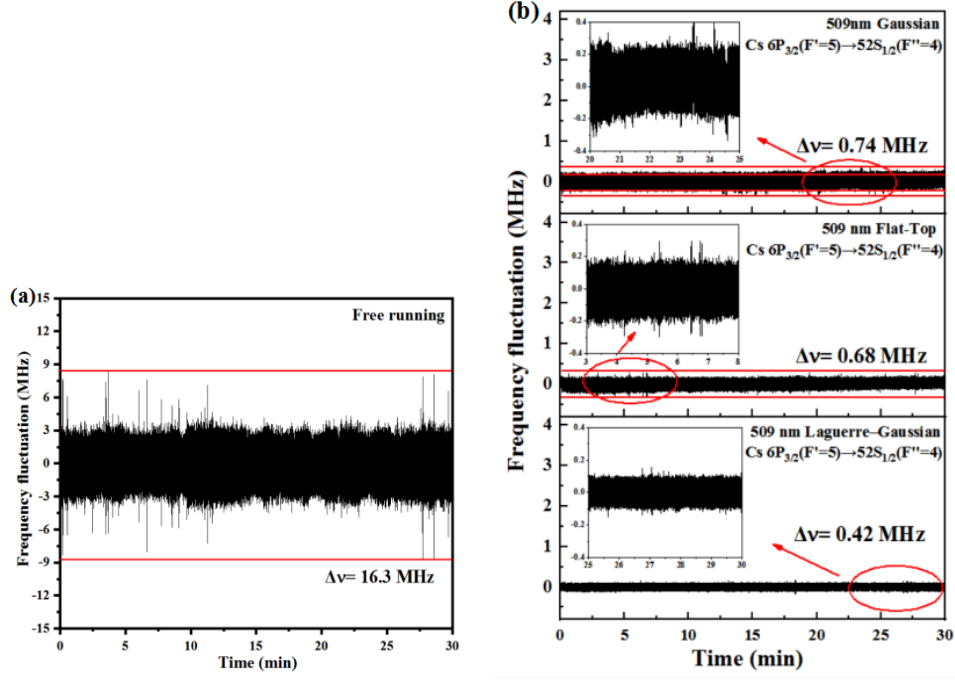
Figure 9: The frequency fluctuation of the 509 nm laser before and after being locked to $6P_{3/2}$(F'=5)-$52S_{1/2}$ Rydberg transition via TCPS scheme. (a) Typical frequency fluctuation of the 509-nm laser in the free running case is about 16.3 MHz. (b) The 509-nm laser is locked to the TCPS with TEM_{00}-mode Gaussian, flat-top, and Laguerre-Gaussian coupling beams, respectively. The corresponding residual frequency fluctuations in 30 minutes are 0.74 MHz, 0.68 MHz, and 0.42 MHz, respectively. The larger the slope of TCPS resonance, the better the 510-nm coupling laser frequency stability after being locked.

4   Conclusion

In conclusion, the EIT and TCPS were investigated for the ladder-type cesium three level system (852 nm + 509 nm) with Rydberg state, the 509-nm coupling beam with three different spatial intensity profile (TEM_{00}-mode Gaussian beam, flat-top beam, and Laguerre-Gaussian beam) was employed. The TCPS frequency difference between the troughs and peaks can easily calibrate the linewidth of the EIT without considering the transmittance. We calibrated the Rabi frequency of the beams with three spatial intensity distributions using A-T splitting, and the 509 nm coupling beam of the Laguerre-Gaussian mode performed the narrowest linewidth EIT at the same Rabi frequency, which is due to the unique spatial mode and reduces the optical pumping effect in the EIT spectra. We optimized the spectrum by changing the size of the Laguerre-Gaussian beam, the narrow linewidth and high contrast EIT have important applications in laser frequency stabilization, microwave electric field probing, Rydberg atomic antenna and Rydberg atomic microwave radar. Finally, we compared the frequency stability of the 509 nm laser frequency locked to the TCPS with different slopes.

Conflict of Interest
The authors declare no conflict of interest.

Data Availability Statement
The data that support the findings of this study are available from the corresponding author upon reasonable request.

References

[1] S. E. Harris, "Lasers without inversion: Interference of lifetime-broadened resonances," Physical Review Letters 62, 1033 (1989).

[2] J. E. Field, K. H. Hahn, and S. E. Harris, "Observation of electromagnetically induced transparency in collisionally broadened lead vapor," Physical Review Letters 67, 3062 (1991).

[3] K. J. Boller, A. Imamoğlu, and S. E. Harris, "Observation of electromagnetically induced transparency," Physical Review Letters 66, 2593 (1991).

[4] A. Kasapi, M. Jain, G. Y. Yin, and S. E. Harris, "Electromagnetically induced transparency: propagation dynamics," Physical Review Letters 74, 2447 (1995).

[5] M. M. Kash, V. A. Sautenkov, A. S. Zibrov, L. Hollnerg, G. R. Welch, M. D. Luckin, Y. Rostovtsev, E. S. Fry, and M. O. Scully, "Ultraslow group velocity and enhanced nonlinear optical effects in a coherently driven hot atomic gas," Physical Review Letters 82, 5229 (1999).

[6] O. Schmidt, R. Wynands, Z. Hussein, and D. Meschede, "Steep dispersion and group velocity below c 3000 in coherent population trapping," Physical Review A 53, R27 (1996).

[7] J. Gea-Banacloche, Y. Li, S. Jin, and M. Xiao, "Electromagnetically induced transparency in ladder-type inhomogeneously broadened media: Theory and experiment," Physical Review A 51, 576 (1995).

[8] Y. Li and M. Xiao, "Electromagnetically induced transparency in a three-level Λ-type system in rubidium atoms," Physical Review A 51, R2703 (1995).

[9] M. Xiao, Y. Li, S. Jin and J. Gea-Banacloche, "Measurement of dispersive properties of electromagnetically induced transparency in rubidium atoms," Physical Review Letters 74, 666 (1995).

[10] A. K. Mohapatra, T. R. Jackson, and C. S. Adams, "Coherent optical detection of highly excited Rydberg states using electromagnetically induced transparency," Physical Review Letters 98, 113003 (2007).

[11] H. S. Moon, L. Lee, K. Kim, and J. B. Kim, "Laser frequency stabilizations using electromagnetically induced transparency," Applied Physics Letters 84, 3001-3003 (2004).

[12] M. Mack, F. Karlewski, H. Hattermann, S. Höckh, F. Jessen, D. Cano, and J. Fortágh, "Measurement of absolute transition frequencies of ^{87}Rb to nS and nD Rydberg states by means of electromagnetically induced transparency," Physical Review A 83, 052515 (2011).

[13] C. Liu, Z. Dutto, C. H. Behroozi, and L. V. Hau, "Observation of coherent optical information storage in an atomic medium using halted light pulses," Nature 409: 490-493 (2001).

[14] Q. Q. Niu, N. Su, Y. Liu, X. J. Ban, J. He, and J. M. Wang, "Rydberg atomic two-color polarization spectroscopy laser frequency stabilization," Journal of Quantum Optics 29: 031001 (2023) (in Chinese).

[15] C. Wieman and T. W. Hänsch, "Doppler-free laser polarization spectroscopy," Physical Review Letters 36, 1170 (1976).

[16] H. B. Lu, X. Y. Wang, H. M. Yan, and Y. Z. Wang, "^{85}Rb atomic polarization spectral stabilized Ti Sapphire laser," Journal of Optoelectronicsd·Laser 11, 573-575 (2000) (in Chinese).

[17] J. Wang, J. Gao, B. D. Yang, T. C. Zhang, and J. M. Wang, "Comparison of Rubidium saturation absorption spectra and polarization spectra for frequency stabilization of a 780-nm diode laser," Chinese Optics 4, 305-312 (2011) (in Chinese).

[18] H. F. Liu, J. Wang, G. Yang, B. D. Yang, J. He, and J. M. Wang, "Two-photon polarization spectroscopy of rubidium $4D_{5/2}$ state and its application for frequency stabilization of 1.5 μm laser," Chinese Journal of Lasers 41(7), 715004–1 (2014) (in Chinese).

[19] N. Duarte Gomes, B. da Fonseca Magnani, J. D, Massayuki Kondo, and L. G. Marcassa, "Polarization spectroscopy applied to electromagnetically induced transparency in hot Rydberg atoms using a Laguerre–Gaussian Beam," Atoms 10, 58 (2022).

[20] A. Chopinaud, and J. Pritchard, "Optimal state choice for Rydberg-atom microwave sensors," Physical Review Applied 16, 024008 (2021).

[21] D. Anderson, R. Sapiro, L. Gonçalves, R. Cardman, and G. Raithel, "Optical radio-frequency phase measurement with an internal-state Rydberg atom interferometer," Physical Review Applied 17, 044020 (2022).

[22] J. Anupriya, N. Ram, and M. Pattabiraman, "Hanle electromagnetically induced transparency and absorption resonances with a Laguerre Gaussian beam," Physical Review A 81, 043804 (2010).

[23] S. R. Chanu, and V. Natarajan, "Narrowing of resonances in electromagnetically induced transparency and absorption using a Laguerre–Gaussian control beam," Optics Communications 295, 150–154 (2013).

[24] V. S. Chauhan, R. Kumar, D. Manchaiah, P. Kumar, and R. K. Easwaran, "Narrowing of electromagnetically induced transparency by using structured coupling light in ^{85}Rb atomic vapor medium," Laser Physics 30, 065203 (2020).

[25] T. Akin, S. Krzyzewski, A. Marino, and E. Abraham, "Electromagnetically induced transparency with Laguerre–Gaussian modes in ultracold rubidium," Optics Communications 339, 209–215 (2015).

[26] T. Akin, S. Krzyzewski, M. Holtfrerich, and E. Abraham, "Optimization of electromagnetically induced transparency by changing the radial size of Laguerre–Gaussian laser modes," Journal of the Optical Society of America B 34, 1286–1293 (2017).

[27] C. Carr, C. S. Adams, and K. J. Weatherill, "Polarization spectroscopy of an excited state transition," Optics Letters 37, 118-120 (2012).

[28] D. H. Meyer, P. D. Kunz, and N. Solmeyer, "Nonlinear polarization spectroscopy of a Rydberg state for laser stabilization," Applied Optics 56(3), B92-B96 (2017).